Direct O2 Activation on Gold/Metal Oxide Catalysts through a Unique Double Linear OAuO Structure

4 AUTHORS, INCLUDING:

Keju Sun
National Institute of Advanced Industrial Sc…
28 PUBLICATIONS **488** CITATIONS

SEE PROFILE

Masanori Kohyama
National Institute of Advanced Industrial Sc…
152 PUBLICATIONS **1,533** CITATIONS

SEE PROFILE

Direct O₂ Activation on Gold/Metal Oxide Catalysts through a Unique Double Linear O—Au—O Structure

Keju Sun,*[a, b] Masanori Kohyama,[a] Shingo Tanaka,[a] and Seiji Takeda[b]

Nanogold particles supported on metal oxide surfaces present unusually high catalytic performances in low-temperature oxidation reactions. Despite numerous studies on that matter, the molecular mechanism concerning O₂ activation remains controversial. Aimed to identify the active sites for direct O₂ activation on gold, a Au—O—O—Au structure was analyzed by Hückel theory. It was found that an increase of Au–O orbital interaction can significantly promote O₂ adsorption and dissociation. Therefore, we constructed a realistic model with a unique double linear O_s–Au–O_a structure at the perimeter of the Au/metal oxide interfaces, which was examined subsequently by DFT calculations. The double linear O_s–Au–O_a structure exhibited high reactivity, with O₂ dissociation barriers as low as 0.12 eV and 0.17 eV for Au/TiO₂ and Au/CeO₂ systems, respectively. The present work gives new insight into the reaction mechanism of low-temperature oxidation reactions on gold catalysts.

Introduction

In recent years, the mechanism of extraordinary low temperature oxidation reactions mediated by nanogold catalysts has been widely studied[1–6] because of their potential applications in the chemical industry for oxidation reactions[1,7–9] and selective oxidation reactions.[10–12] The central topic in the mechanism of gold-catalyzed oxidation reactions is the activation/dissociation of O₂,[13] which represents a major challenge. Despite numerous studies conducted on that matter, it remains controversial how O₂ is activated on the Au/metal oxide. Theoretical calculations[5,6,13–18] indicated a direct O₂ dissociation on the gold/metal oxide with a very high activation barrier, in spite of experimental results that the apparent activation energy is very low, usually below 40 kJ mol⁻¹ and sometimes even below 10 kJ mol⁻¹.[19] Furthermore, the reaction of CO with molecularly chemisorbed oxygen on gold was found to be relatively facile,[5,16,20,21] and a mechanism of O₂ activation with the help of co-adsorbed CO was suggested by theoretical results. However, this viewpoint of indirect O₂ activation was challenged by some experimental results.

Based on a comparison of the reduction rate of preoxidized Au/TiO₂ samples by CO with the rate of the catalytic oxidation of CO on Au/TiO₂ catalysts, it was suggested that O₂ is directly activated.[22] Furthermore, in situ X-ray adsorption near-edge structure studies have revealed that gold nanoparticles in Au/metal oxide catalysts are oxidized if exposed to oxygen pressure,[23,24] providing strong evidence for direct O₂ activation. Results from temporal analysis of products experiments[25,26] also demonstrate that the active oxygen species can be formed on Au/TiO₂ catalysts at 80 °C by exposure to thermal O₂ pulses. Using in situ environmental TEM, Uchiyama et al. gave more direct evidence.[27] They observed that the morphology of gold nanoparticles supported on CeO₂ changed to a rounder shape after pure O₂ gas was induced, indicating that O₂ molecules were dissociated into atomic oxygen or active oxygen species. In addition, owing to the high stability of the active oxygen species (up to at least 400 °C), this species was suggested to be atomic, formed by adsorption, activation, and dissociation of molecular oxygen.[26] All in all, these experiments clearly reveal that O₂ can be activated directly without the presence of CO on supported gold systems. In spite of these experimental results, theoretical results hold an indirect O₂ activation mechanism. This contradiction can be explained by the fact that the active sites examined in previous theoretical studies may not be identical to those actually involved in the reaction, thereby leading to an overestimation of the barrier of direct O₂ dissociation.

Although DFT calculation is a powerful tool for various systems and provides enough accuracy to be compared to experimental data, it is not necessarily good at predicting the tendency of some chemical phenomena, because of the nature of DFT theory relying only on the electron density as well as numerical complexities. On the other hand, Hückel theory is not a quantitative theory, but it can grasp the essence and tendency of chemical phenomena, and, hence, provide some interesting and valuable predictions. Therefore, a combination of Hückel theory and DFT calculations was expected to be a powerful method in computational physics and chemistry. Our previous studies demonstrated the potential of complementary combination between Hückel theory and DFT calculations to

[a] Dr. K. Sun, Dr. M. Kohyama, Dr. S. Tanaka
Research Institute for Ubiquitous Energy Devices
National Institute of Advanced Industrial Science and Technology
1-8-31, Midorigaoka, Ikeda, Osaka 563-8577 (Japan)
Fax: (+81) 72-751-9714
E-mail: keju.sun@aist.go.jp

[b] Dr. K. Sun, Prof. Dr. S. Takeda
The Institute of Scientific and Industrial Research
Osaka University
8-1 Mihogaoka, Ibaraki, Osaka 567-0047 (Japan)

Supporting information for this article is available on the WWW under
http://dx.doi.org/10.1002/cctc.201300134.

understand CO and atomic oxygen adsorption on various gold systems.[28,29] Herein, we aimed at identifying the active sites for direct O_2 activation with lower energy barrier and, therefore, we investigated the O_2 dissociation on both gold surfaces and gold/metal oxide systems by a combination of Hückel theory[30,31] and DFT calculations. On the basis of Hückel theory analysis, we then proposed site with a unique double linear O—Au—O structure at the perimeter of Au/metal oxide interface. Subsequent DFT calculations revealed that the unique double linear O—Au—O structure is highly active for O_2 dissociation. These results are in good agreement with recent experimental results and provide new insight into the reaction mechanism of low-temperature oxidation reactions on gold catalysts.

Results and Discussion

Prediction by Hückel theory

Firstly, O_2 dissociation on gold was analyzed by Hückel theory. A simple model containing only four atoms was constructed as shown in Figure 1 a. Similarly to atomic oxygen adsorption[28] and CO adsorption[29] on Au surfaces, the orbital interaction in the Au—O—O—Au structure could be separated into two parts: the σ-bonding contribution and the π-bonding contribution. For the σ-bonding, two electrons come from each O atom and two electrons come from each Au atom,[28] therefore, all bonding and antibonding orbitals are fully filled. As a result, the contribution of the σ-bonding can be neglected, and the dominant contribution is assigned to the π-bonding. Thus, we only focused on the contribution of π-bonding.

The π-bonding wave function in the Au—O—O—Au structure is expressed as

$$\Psi = c_1\varphi_1 + c_2\varphi_2 + c_3\varphi_3 + c_4\varphi_4 \tag{1}$$

The basic secular determinant is given as

$$\begin{vmatrix} \alpha_{Au} - E & \beta_{O-Au} & 0 & 0 \\ \beta_{O-Au} & \alpha_O - E & \beta_{O-O} & 0 \\ 0 & \beta_{O-O} & \alpha_O - E & \beta_{O-Au} \\ 0 & 0 & \beta_{O-Au} & \alpha_{Au} - E \end{vmatrix} = 0 \tag{2}$$
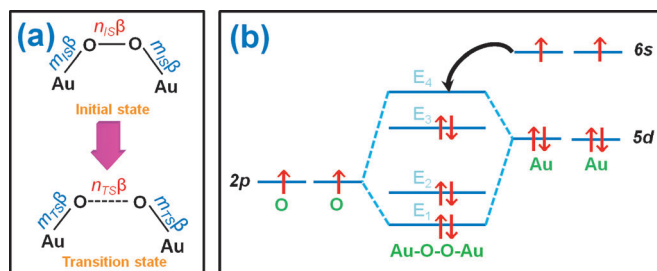

Figure 1. a) The model of orbital interactions in an Au—O—O—Au configuration for the initial and the transition states and b) π-electron distribution in Au—O—O—Au molecular orbitals.

The parameters of β_{O-Au} and β_{O-O} represent the O—Au and O—O π-orbital interactions. The parameters of α_O and α_{Au} are the values of relevant Coulomb integrals for O and Au atoms, respectively. If we assume the relations as $\alpha_{Au} = \alpha$, $\beta_{O-Au} = m\beta$, $\beta_{O-O} = n\beta$ and $\alpha_O = \alpha + h\beta$, the solutions of the secular determinant for the Au—O—O—Au structure are given by (see the Supporting Information for the seeking process),

$$\begin{cases} E_1 = \alpha - \frac{-(h+n)-\sqrt{(h+n)^2+4m^2}}{2}\beta \\ E_2 = \alpha - \frac{-(h-n)-\sqrt{(h-n)^2+4m^2}}{2}\beta \\ E_3 = \alpha - \frac{-(h+n)+\sqrt{(h+n)^2+4m^2}}{2}\beta \\ E_4 = \alpha - \frac{-(h-n)+\sqrt{(h-n)^2+4m^2}}{2}\beta \end{cases} \quad (E_1 \le E_2 \le E_3 \le E_4) \tag{3}$$

For these π-bonding orbitals, two electrons come from two O atoms and four electrons come from two Au atoms, and in this way there are six electrons in each π-bonding orbital. The π-electron distribution in the Au—O—O—Au molecular orbitals is shown in Figure 1 b. Therefore, the contribution of each π-bond formation is given as

$$\Delta E_\pi = 2E_1 + 2E_2 + 2E_3 - 4\alpha_{Au} - 2\alpha_O$$
$$= (h + n + \sqrt{(h-n)^2 + 4m^2})\beta \tag{4}$$

Assuming m and n at the initial state (IS) changed to $m + \Delta m$ and $n - \Delta n$ at the transition state (TS) ($\Delta m > 0$, $\Delta n > 0$), we can obtain the total energies for IS and TS as

$$E_{IS} = 2(h + n + \sqrt{(h-n)^2 + 4m^2})\beta \tag{5}$$

$$E_{TS} = 2(h + n - \Delta n + \sqrt{(h-n+\Delta n)^2 + 4(m+\Delta m)^2})\beta \tag{6}$$

Notably, IS corresponds to the state of O_2 molecular adsorption and the state called FS corresponds to the state of dissociated oxygen adsorption. Assuming n, Δm and Δn are independent from m, we can conclude from Equations (5) and (6) that both E_{IS} and E_{TS} will decrease with the increase of m, as β is negative. The decrease of E_{IS} or E_{TS} means that the structures at IS and TS are more stable. The reaction barrier for O—O dissociation is expressed as

$$E_{barrier} = E_{TS} - E_{IS}$$
$$= 2(-\Delta n + \frac{2(\Delta n)(h-n) + (\Delta n)^2 + 8(\Delta m)m + 4(\Delta m)^2}{\sqrt{(h-n)^2+4m^2} + \sqrt{(h-n+\Delta n)^2+4(m+\Delta m)^2}})\beta \tag{7}$$

As n, Δm, and Δn are independent from m, it is very convenient to obtain the relation ($\partial E_{barrier}/\partial m < 0$). As a result, $E_{barrier}$ also decreases with the increase of m. This indicates that the influence of m on E_{TS} is stronger than that on E_{IS}. In this way, all the values of E_{IS}, E_{TS}, and $E_{barrier}$ decrease with the increase of m. More specifically, the O_2 adsorption on gold surfaces will be

strengthened, and the barrier for O_2 dissociation will be reduced if m is increased.

Herein, direct O_2 dissociation is described by the unimolecular decomposition mechanism

$$O_2(gas) \xrightleftharpoons{K_{O_2}} O_2(ads) \xrightarrow{k_2} 2O(ads) \tag{8}$$
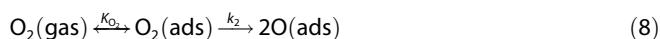
in which K_{O_2} is the equilibrium constant of adsorption and k_2 is the rate constant. According to the rate equation for O_2 dissociation and Langmuir equation, the dissociation rate r can be given by the mechanism

$$r = -\frac{d[O_2(ads)]}{dt} = k_2 \theta_{O_2} = k_2 \frac{K_{O_2} P_{O_2}}{K_{O_2} P_{O_2} + 1} \tag{9}$$

in which θ_{O_2} is the coverage of adsorbed O_2 on surfaces, and P_{O_2} is the pressure of O_2. If the pressure of O_2 is low,

$$r \approx k_2 K_{O_2} P_{O_2} \tag{10}$$

According to Arrhenius law and van't Hoff relationship,

$$\frac{d \ln(r)}{dT} = \frac{d \ln k_2}{dT} + \frac{d \ln K_{O_2}}{dT} = \frac{E_{barrier}}{RT^2} + \frac{E_{IS}}{RT^2} = \frac{E_{barrier} + E_{IS}}{RT^2} \tag{11}$$

in which R is the gas constant and T is the temperature. Thus, the apparent activation energy at low pressure is $E_{barrier} + E_{IS}$. If the pressure of O_2 gas is high,

$$r \approx k_2 \tag{12}$$

and

$$\frac{d \ln(r)}{dT} = \frac{d \ln k_2}{dT} = \frac{E_{barrier}}{RT^2} \tag{13}$$

The apparent activation energy at high pressures is $E_{barrier}$. As discussed above, both E_{IS} and $E_{barrier}$ decrease if the interaction between Au and O orbitals, namely the value of m, increases. Thus O_2 is activated more easily if m is increased, regardless of the pressure.

The kernel of the problem is how to increase the Au–O orbital interaction, namely the value of m. Our previous study[28] has demonstrated that the linear O–Au–O structure significantly increases the interaction between Au and O, and strongly increases the value of m. In addition, the stability of O–Au–O was also confirmed by Frondelius et al.[32] Therefore, the sites at which the linear O–Au–O structure is easily formed should be favorable for the O_2 adsorption and dissociation. Our previous study[28] also showed that the interaction between O and Au can be enhanced if the coordinate number of oxygen is increased. In practice, owing to limitation of the surface structure, it is not very convenient to increase the coordinate number remarkably. Therefore, promotion of O_2 activation only from the linear O–Au–O structure is discussed in this article.

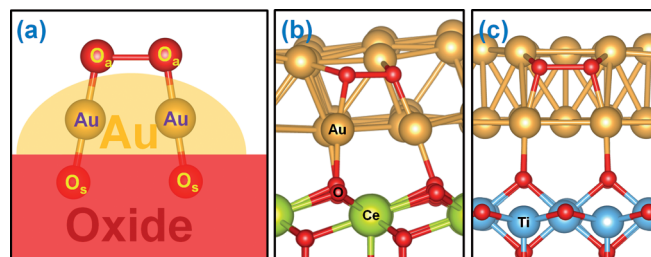Based on these considerations, we proposed a model configuration of a Au/metal oxide system with Au atoms at the pe-

Figure 2. A model of the unique double linear O_s-Au-O_a structure (a) and realistic configurations of the double linear O–Au–O structure at the perimeter of Au/CeO$_2$-L (b) and Au/TiO$_2$-L (c). The corresponding configurations are the O_2 dissociation structures at the transition states.

rimeter in contact with O atoms in the substrate surface. As shown in Figure 2a, a unique double linear O_s–Au–O_a structure can be formed with an adsorbed oxygen molecule at the perimeter. Here O_s and O_a indicate the surface oxygen atom in the metal oxide substrate and the adsorbed molecular O_2, respectively. The gold atom in the O_s–Au–O_a structure is located at the perimeter of the gold cluster deposited on the oxide surface. At the perimeter of the Au/metal oxide interface with numerous Au atoms, such double linear O_s–Au–O_a structures can be easily formed with an adsorbed oxygen molecule, because the on-top sites of surface oxygen atoms in oxide surfaces are the favored sites for the interface Au atoms (see Table S1 in the Supporting Information). In Figure 2b and 2c, examples of realistic configurations of the unique double O_s–Au–O_a structure are shown, which have a high activity for O_2 dissociation in the Au/CeO$_2$ system and Au/TiO$_2$ system.

Above we described the contributions of the 5d electrons to the Au–O–O–Au molecule, and it was concluded that increase of m could promote O_2 activation. Next we discuss the influence of the 6s electron of the gold to O_2 activation. Similarly to the contribution of the 6s electron to the Au–O molecule,[28] the 6s electron of gold could transfer to the Au–O–O–Au orbital, because the antibonding orbital is not fully filled (see Figure 1b). The system will be more stable because of the energy gain from the transfer of the 6s electron, and, hence, E_{IS} and E_{TS} will be decreased (more stable) involving the contribution of the 6s electron. In addition, as the decrease of the energy owing to the 6s electron transfer occurs at the IS and TS simultaneously, the influence of electron transfer to the reaction barrier will not be remarkable. Therefore, Hückel theory predicts that the co-adsorbed or doped electron donor/accepter, which promotes/hinders electron transfer to O_2, can strengthen/weaken O_2 adsorption correspondingly. However, the influence of the electron donor or accepter to the reaction barrier will be relatively weak.

Examination by DFT calculations

To verify the prediction about the influence of the electron donor/acceptor by Hückel theory, O_2 adsorption and dissociation on the Au(100) surface with and without co-adsorbed Na (denoted as Au(100)_Na) or Cl (denoted as Au(100)_Cl) atom was calculated by DFT calculations. The corresponding energies and structures are shown in Table 1 and Figure S1. Bader

Table 1. The O_2 adsorption energies before (IS) and after dissociation (FS) and the reaction barriers (TS) in different Au slab surfaces, Au rod surfaces, and Au/metal oxide interfaces, in eV.

	E_{ads} (IS)	$E_{barrier}$ (TS)	E_{ads} (FS)
Au(100)	0.03	0.50	0.30
Au(100)_Na	−0.07	0.52	0.16
Au(100)_Cl	0.11	0.48	0.34
Au(111)	0.51	0.99	0.00
Au(321)	0.31	0.88	0.26
Au(711)	−0.19	0.64	0.26
Au_rod(111)	0.22	0.83	−0.56
Au_rod(100)	−0.31	0.44	−0.49
Au/CeO$_2$-NL	0.00	0.50	−1.61
Au/CeO$_2$-L	−0.31	0.17	−1.16
Au/TiO$_2$-L	0.38	0.12	−0.11
Au/MgO-L	−0.34	0.39	−1.71

charge analysis revealed that the electron participations on the adsorbed O_2 are 0.77, 0.81, and 0.76 at IS; and 1.09, 1.11, and 1.07 at TS; on Au(100), Au(100)_Na, and Au(100)_Cl, respectively. This result shows that sodium as an electron donor promotes the electron transfer to O_2, whereas chlorine as an electron acceptor hinders it. According to the prediction from Hückel theory, charge transfer to O_2 will promote O_2 adsorption. Furthermore, O_2 adsorption is strengthened by 0.10 eV with co-adsorbed sodium. However, it is weakened by 0.08 eV in the presence of co-adsorbed chlorine. Thus, the DFT calculations clearly certified the prediction by Hückel theory that the electron donor strengthens the O_2 adsorption, whereas the electron accepter weakens it.

Our DFT calculations also revealed that the barriers for O_2 dissociation on Au(100), Au(100)_Na, and Au(100)_Cl are 0.50 eV, 0.52 eV, and 0.48 eV, respectively. Compared to the variation of adsorption energies of 0.08–0.18 eV, the barrier difference in the range of 0.02–0.04 eV among the three surfaces is much smaller. These results show that the electron donor/acceptor affects the adsorption energy more than the reaction barrier, which is in good agreement with the prediction by Hückel theory. It should be noted that the variation of the reaction barrier owing to the electron donor or acceptor is only 0.02–0.04 eV, which is almost in the margin of the DFT error. Therefore, the influence of the electron donor or accepter to the reaction barrier is very weak and can be ignored in most cases.

To testify that the unique double linear O—Au—O structure is highly active for O_2 activation as predicted by Hückel theory, we performed a comparative study of O_2 dissociation on gold surfaces and perimeters of gold/metal oxide systems by DFT calculations. The corresponding structures are shown in Figure S1–S8 and the energies are listed in Table 1. It was found that Au(100) on gold rod (Au_rod(100)) with the barrier of 0.44 eV is the most active among Au surfaces and Au clusters (rods), which agrees well with other calculation results.[13, 33, 34] However, it is less reactive than the Au/TiO$_2$-L, Au/CeO$_2$-L and Au/MgO-L systems that have barriers of 0.12, 0.17, and 0.39 eV, respectively. In all the three Au/metal oxide system, the unique double linear O$_s$—Au—O$_a$ structure is formed and denoted as

"-L". To make certain this activation stems from the linear O—Au—O structure and not from the perimeter effect, O_2 dissociation at the perimeter of Au/CeO$_2$-NL system without the formation of linear O—Au—O structure (denoted as "-NL") was also calculated. Only the energetically favorable structure among all the Au/CeO$_2$-NL structures is shown in Figure S5. It was found that the O_2 adsorption energy is 0.00 eV at the perimeter of the Au/CeO$_2$-NL system, which is weaker than that of the Au/CeO$_2$-L system by 0.31 eV. The O_2 dissociation barrier at the perimeter of Au/CeO$_2$-NL system is higher than that of Au/CeO$_2$-L system by 0.33 eV. This result clearly shows that the formation of the unique double linear O$_s$—Au—O$_a$ structure enhance the O_2 adsorption and dissociation, because the linear O$_s$—Au—O$_a$ structure strengthens the Au—O interaction, as predicted by Hückel theory.

As summarized in Table 1, the Au/CeO$_2$-L system with the double linear O$_s$—Au—O$_a$ structure is very reactive for O_2 activation with an adsorption energy of −0.31 eV and a dissociation barrier of 0.17 eV. The lowest barrier with 0.12 eV is found on Au/TiO$_2$-L system among all the Au surfaces and Au/metal oxide systems considered. However, we note that the adsorption energy of O_2 on Au/TiO$_2$-L is as high as 0.38 eV, which is disfavored for O_2 activation. The high adsorption energy should be assigned to the charge effect. Bader analysis shows the Au rods with 0.11, −1.30, and 1.09 electrons in Au/CeO$_2$-L, Au/TiO$_2$-L, and Au/MgO-L respectively. Clearly, more electrons are transferred from Au rods to TiO$_2$, and the Au rod in Au/TiO$_2$-L loses 1.30 electrons. As we discussed above, the effect of electrons transfer from Au to TiO$_2$ is equivalent to that of Au co-adsorption with electron acceptors, which will lead to weak O_2 adsorption. Therefore, the adsorption energy of O_2 on Au/TiO$_2$-L is as high as 0.38 eV.

It should be noted that the electron-transfer direction in our DFT calculation was against that in the experimental results,[35–37] which exhibited an electron transfer from TiO$_2$ to Au clusters. This difference between theoretical and experimental results can be explained as follows. First, the TiO$_2$ surfaces used in the experimental studies were defected surfaces with oxygen vacancies or hydroxyl groups, whereas the TiO$_2$ surface in our DFT calculations was a stoichiometric surface. And second, more importantly, the generalized gradient approximation functional missed a term coming from the discontinuity of derivatives of the exchange correction functional, which plays a critical role in the correct prediction of band gaps and charge-transfer systems.[38] Therefore, the DFT results about the charge-transfer direction between Au cluster and metal oxide are dubious. Considering the experimental electron transfer from TiO$_2$ to Au, the TiO$_2$ should act as an electron donor, so the adsorption of O_2 on Au/TiO$_2$ will be heavily strengthened compared to the DFT results. In other words, the DFT calculations significantly underestimated the binding energy of O_2 on Au/TiO$_2$-L; therefore, the real binding energy (negative adsorption energy) of O_2 on Au/TiO$_2$-L will be much stronger than in the DFT result. Thus, it can be expected that Au/TiO$_2$ with the reaction barrier of 0.12 eV can also be reactive for O_2 dissociation. In addition, as we have discussed before, the apparent activation energy is $E_{barrier}$ at a high pressure. Thus, the Au/TiO$_2$
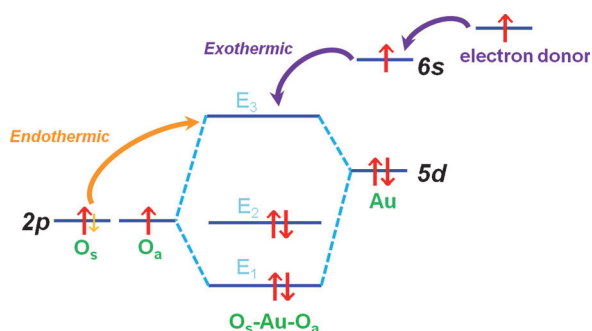
Figure 3. A diagram of the π-electron distribution in O_s–Au–O_a molecular orbitals. An extra electron on O_s is marked by orange color, and its transfer to the E_3 orbital should destabilize the O_s–Au–O_a structure.

system is active, at least in systems with high O_2 partial pressure.

Despite the formation of the double linear O_s–Au–O_a structure, the O_2 dissociation on the Au/MgO-L system has a barrier of 0.39 eV, much higher than the barriers of the Au/TiO$_2$-L and Au/CeO$_2$-L systems (Table 1). According to Hückel theory, this difference can be attributed to the different charges of O_s in different oxides. In Figure 3, the schematic diagram of the π-electron distribution in the O_s–Au–O_a molecular orbitals is shown. If the O_s has more electrons, these electrons will transfer to the antibonding orbital of the O_s–Au–O_a molecule. Unlike the transfer from the 6s orbital of Au or electron donor to the antibonding orbital, which is exothermic, the transfer from O_s is endothermic. As a result, the stability of the linear O–Au–O structure is destroyed and the Au–O interaction is weakened, which leads to a higher barrier for the O_2 dissociation. The partial charge of oxygen in the metal oxides should depend on the electronegativity of the metal ions, which reflects the tendency to attract electrons. The electronegativities of Mg^{2+}, Ti^{4+}, and Ce^{4+} are 6.55, 13.86, and 10.08, respectively, according to Tanaka's method.[39] Therefore, the oxygen ions in MgO have more electrons than those in TiO$_2$ and CeO$_2$. This is also confirmed by the Bader charge analysis in the DFT calculations, which reveals a Bader charge of the surface oxygen in the clean MgO(100) surface of 1.64 electrons, much larger than the values of 0.85 and 1.19 electrons in TiO$_2$(110) and CeO$_2$(111) surfaces, respectively.

To the best of our knowledge, the present dissociation barriers of 0.12 eV and 0.17 eV for Au/TiO$_2$ and Au/CeO$_2$ systems are the lowest among those in the previous literature. The high O_2 dissociation reactivity by the present perimeter models of Au/TiO$_2$ or Au/CeO$_2$ systems indicates the probable mechanism of direct O_2 activation in gold/metal oxide catalysts. The high activity of the perimeter region of Au/metal oxide interfaces is consistent with the experimental findings,[2,25,26,40] particularly concerning the results proposed by Zhou et al. based on their TEM and XRD analyses.[41]

The previous theoretical results in the literature[5,6,13–18] showed that direct O_2 dissociation is hindered by relatively high barriers, and the authors proposed a mechanism of O_2 dissociation with the help of CO molecules. However, herein we found a favorable reaction pathway for the direct O_2 disso-

ciation at the perimeters of Au/TiO$_2$ and Au/CeO$_2$ interfaces with lower barriers. Our DFT calculations also show that the CO reaction with atomic oxygen species is relatively facile with a reaction barrier of only 0.01 eV (see Figure S9), which agrees well with previous studies.[42–44] Therefore, the direct O_2 dissociation mechanism also provides an understanding for the low-temperature CO oxidation on gold catalysts. In addition, the moderate Au–O binding in the O–Au–O structure will make gold catalysts desirable for some other oxidation reactions with high reactivity. Therefore, understanding of the O_2 direct dissociation should help us not only to understand the high activity of gold catalysts, but also to obtain a guide for the design of highly efficient catalysts for oxidation reactions with high selectivities.

Conclusions

The direct O_2 dissociation on Au and Au/metal oxide surfaces was investigated by employing Hückel theory and DFT calculations. Hückel theory analysis showed that stronger O_2 adsorption and lower O_2 dissociation barriers can be achieved by strengthening the Au–O orbital interactions. It is known that a linear O–Au–O structure leads to enhanced Au–O orbital interactions. Thus we have constructed realistic models of the perimeter configurations of Au/metal oxide interfaces with a unique double linear O–Au–O structure, and examined the energies of O_2 adsorption and dissociation by DFT calculations. It was found that, with the unique double linear O–Au–O structure, O_2 dissociation is relatively facile, with barriers as low as 0.12 eV and 0.17 eV for the Au/TiO$_2$-L and Au/CeO$_2$-L systems, respectively. These values are much lower than those for Au surfaces and Au/metal oxide interfaces without the double linear O–Au–O structure, indicating that the unique double linear O–Au–O structure may be the real active site for direct O_2 dissociation. In addition, the low reactivity of the Au/MgO-L system with the double O–Au–O structure can be explained by more oxygen partial electrons on the surface oxygen in a MgO surface, leading to less strengthening of the Au–O interactions in the linear O–Au–O structure. The low O_2 dissociation barrier at the perimeters of Au/TiO$_2$ or Au/CeO$_2$ systems is consistent with recent experimental results, and provides new insight toward low-temperature oxidation reactions on gold catalysts.

Experimental Section

Periodic DFT calculations using the Vienna ab initio simulation package[45] were performed to calculate the O_2 adsorption and dissociation on gold surfaces and gold/metal-oxide systems. The exchange-correlation energy and potential are described by the generalized gradient approximation in the form of Perdew–Burke–Ernzerhof.[46] Plane waves are used to expand wave functions with a cutoff of 400 eV for projector augmented wave potentials.[47,48] The criteria for the convergence in the structural determination were the residual force less than 0.02 eVÅ^{-1}. All slab surfaces including Au(111), Au(100), Au(321) and Au(711) surfaces were modeled by a five-layer slab with a vacuum thickness of 15 Å, in which the adsorbed species are placed on one side. The top three

layers were relaxed, whereas the two bottommost layers were fixed at their bulk structure. A 4×4 supercell was used for Au(111) and Au(100) surfaces with the Monkhorst–Pack (MP) 3×3×1 k-point mesh. For the Au(100) Na or Au(100) Cl system, the co-adsorbed Na or Cl was fixed at the hole site. A 2×2 supercell was used for a Au(321) surface with the MP 2×2×1 k-point mesh. A 1×3 supercell is used for a Au(711) surface with the MP 2×2×1 k-point mesh. To simulate the Au cluster, a gold rod was used with MP 1×2×1 k-point mesh as shown in Figure S10.

Models of Au rod/metal oxide systems were constructed to deal with the perimeter regions.[49] For a Au/MgO system, a gold rod with 20 atoms per period was supported on a 4×4 MgO(001) surface slab with three atomic layers and the MP k-point mesh was 3×3×1. For a Au/TiO$_2$ system, a gold rod with 24 atoms per period was supported on a 2×4 TiO$_2$(110) surface slab with nine atomic layers and the MP k-point mesh was 2×2×1. For a Au/CeO$_2$ system, a gold rod with 32 atoms per period was supported on a 3×6 CeO$_2$(111) surface slab with six atomic layers and the MP k-point mesh was 2×1×1. Because of the strong self-interaction effects from the localized 4f electrons of Ce atoms, the DFT+U approach with U value of 5 eV was used for the Au/CeO$_2$ system.[50,51] The structures of transition states were searched by the force-reversed method.[52] The O$_2$ adsorption energy was defined as $E_{ads} = E(surface+O_2)-E(surface)-E(O_2)$, in which $E(surface+O_2)$ corresponded to the energy of a surface with O$_2$ adsorption, $E(surface)$ was the energy of a clean surface, and the $E(O_2)$ was the energy of an isolated O$_2$ molecule. Spin polarization was considered during all the calculations.

Acknowledgements

[1] M. Valden, X. Lai, D. W. Goodman, *Science* **1998**, *281*, 1647–1650.
[2] M. Haruta, *Catal. Today* **1997**, *36*, 153–166.
[3] M. M. Schubert, S. Hackenberg, A. C. van Veen, M. Muhler, V. Plzak, R. J. Behm, *J. Catal.* **2001**, *197*, 113–122.
[4] C. K. Costello, M. C. Kung, H. S. Oh, Y. Wang, H. H. Kung, *Appl. Catal. A* **2002**, *232*, 159–168.
[5] Z. P. Liu, X. Q. Gong, J. Kohanoff, C. Sanchez, P. Hu, *Phys. Rev. Lett.* **2003**, *91*, 266102.
[6] I. N. Remediakis, N. Lopez, J. K. Norskov, *Angew. Chem.* **2005**, *117*, 1858–1860; *Angew. Chem. Int. Ed.* **2005**, *44*, 1824–1826.
[7] M. Haruta, T. Kobayashi, H. Sano, N. Yamada, *Chem. Lett.* **1987**, *16*, 405–408.
[8] A. S. K. Hashmi, G. J. Hutchings, *Angew. Chem.* **2006**, *118*, 8064–8105; *Angew. Chem. Int. Ed.* **2006**, *45*, 7896–7936.
[9] M. Mavrikakis, P. Stoltze, J. K. Norskov, *Catal. Lett.* **2000**, *64*, 101–106.
[10] M. D. Hughes, Y. J. Xu, P. Jenkins, P. McMorn, P. Landon, D. I. Enache, A. F. Carley, G. A. Attard, G. J. Hutchings, F. King, E. H. Stitt, P. Johnston, K. Griffin, C. J. Kiely, *Nature* **2005**, *437*, 1132–1135.
[11] D. I. Enache, J. K. Edwards, P. Landon, B. Solsona-Espriu, A. F. Carley, A. A. Herzing, M. Watanabe, C. J. Kiely, D. W. Knight, G. J. Hutchings, *Science* **2006**, *311*, 362–365.
[12] J. J. Bravo-Suarez, K. K. Bando, J. I. Lu, M. Haruta, T. Fujitani, S. T. Oyama, *J. Phys. Chem. C* **2008**, *112*, 1115–1123.
[13] M. Boronat, A. Corma, *Dalton Trans.* **2010**, *39*, 8538–8546.
[14] B. Yoon, H. Hakkinen, U. Landman, *J. Phys. Chem. A* **2003**, *107*, 4066–4071.
[15] Y. Xu, M. Mavrikakis, *J. Phys. Chem. B* **2003**, *107*, 9298–9307.
[16] L. M. Molina, M. D. Rasmussen, B. Hammer, *J. Chem. Phys.* **2004**, *120*, 7673–7680.
[17] S. Laursen, S. Linic, *J. Phys. Chem. C* **2009**, *113*, 6689–6693.
[18] J. L. C. Fajin, M. N. D. S. Cordeiro, J. R. B. Gomes, *J. Phys. Chem. C* **2007**, *111*, 17311–17321.
[19] M. Haruta, *Cattech* **2002**, *6*, 102–115.
[20] N. Lopez, J. K. Norskov, *J. Am. Chem. Soc.* **2002**, *124*, 11262–11263.
[21] Z. P. Liu, P. Hu, A. Alavi, *J. Am. Chem. Soc.* **2002**, *124*, 14770–14779.
[22] Y. Iizuka, T. Tode, T. Takao, K. Yatsu, T. Takeuchi, S. Tsubota, M. Haruta, *J. Catal.* **1999**, *187*, 50–58.
[23] J. A. van Bokhoven, C. Louis, J. T. Miller, M. Tromp, O. V. Safonova, P. Glatzel, *Angew. Chem.* **2006**, *118*, 4767–4770; *Angew. Chem. Int. Ed.* **2006**, *45*, 4651–4654.
[24] N. Weiher, A. M. Beesley, N. Tsapatsaris, L. Delannoy, C. Louis, J. A. van Bokhoven, S. L. M. Schroeder, *J. Am. Chem. Soc.* **2007**, *129*, 2240–2241.
[25] M. Kotobuki, R. Leppelt, D. A. Hansgen, D. Widmann, R. J. Behm, *J. Catal.* **2009**, *264*, 67–76.
[26] D. Widmann, R. J. Behm, *Angew. Chem.* **2011**, *123*, 10424–10428; *Angew. Chem. Int. Ed.* **2011**, *50*, 10241–10245.
[27] T. Uchiyama, H. Yoshida, Y. Kuwauchi, S. Ichikawa, S. Shimada, M. Haruta, S. Takeda, *Angew. Chem.* **2011**, *123*, 10339–10342; *Angew. Chem. Int. Ed.* **2011**, *50*, 10157–10160.
[28] K. J. Sun, M. Kohyama, S. Tanaka, S. Takeda, *J. Phys. Chem. A* **2012**, *116*, 9568–9573.
[29] K. J. Sun, M. Kohyama, S. Tanaka, S. Takeda, *J. Comput. Chem.* **2011**, *32*, 3276–3282.
[30] E. Hückel, *Z. Angew. Phys.* **1931**, *70*, 204–286.
[31] R. Hoffmann, *J. Chem. Phys.* **1963**, *39*, 1397–1412.
[32] P. Frondelius, H. Hakkinen, K. Honkala, *Angew. Chem.* **2010**, *122*, 8085–8088; *Angew. Chem. Int. Ed.* **2010**, *49*, 7913–7916.
[33] A. Roldan, J. M. Ricart, F. Illas, *Theor. Chem. Acc.* **2009**, *123*, 119–126.
[34] J. Greeley, J. Rossmeisl, A. Hellman, J. K. Norskov, *Z. Phys. Chem. (Muenchen Ger.)* **2007**, *221*, 1209–1220.
[35] T. Minato, T. Susaki, S. Shiraki, H. S. Kato, M. Kawai, K. I. Aika, *Surf. Sci.* **2004**, *566*, 1012–1017.
[36] H. J. Chung, A. Yurtsever, Y. Sugimoto, M. Abe, S. Morita, *Appl. Phys. Lett.* **2011**, *99*, 123102.
[37] Z. Q. Jiang, W. H. Zhang, L. Jin, X. Yang, F. Q. Xu, J. F. Zhu, W. X. Huang, *J. Phys. Chem. C* **2007**, *111*, 12434–12439.
[38] W. T. Yang, A. J. Cohen, P. Mori-Sanchez, *J. Chem. Phys.* **2012**, *136*, 204111.
[39] K. I. Tanaka, A. Ozaki, *J. Catal.* **1967**, *8*, 1.
[40] T. Fujitani, I. Nakamura, *Angew. Chem.* **2011**, *123*, 10326–10329; *Angew. Chem. Int. Ed.* **2011**, *50*, 10144–10147.
[41] Z. Zhou, S. Kooi, M. Flytzani-Stephanopoulos, H. Saltsburg, *Adv. Funct. Mater.* **2008**, *18*, 2801–2807.
[42] J. L. C. Fajin, M. N. D. S. Cordeiro, J. R. B. Gomes, *J. Phys. Chem. C* **2008**, *112*, 17291–17302.
[43] B. K. Min, A. R. Alemozafar, D. Pinnaduwage, X. Deng, C. M. Friend, *J. Phys. Chem. B* **2006**, *110*, 19833–19838.
[44] V. A. Bondzie, S. C. Parker, C. T. Campbell, *Catal. Lett.* **1999**, *63*, 143–151.
[45] G. Kresse, J. Hafner, *Phys. Rev. B* **1993**, *48*, 13115–13118.
[46] J. P. Perdew, K. Burke, M. Ernzerhof, *Phys. Rev. Lett.* **1996**, *77*, 3865–3868.
[47] P. E. Blochl, *Phys. Rev. B* **1994**, *50*, 17953–17979.
[48] G. Kresse, D. Joubert, *Phys. Rev. B* **1999**, *59*, 1758–1775.
[49] H. Q. Shi, M. Kohyama, S. Tanaka, S. Takeda, *Phys. Rev. B* **2009**, *80*, 155413.
[50] D. A. Andersson, S. I. Simak, B. Johansson, I. A. Abrikosov, N. V. Skorodumova, *Phys. Rev. B* **2007**, *75*, 035109.
[51] C. Loschen, J. Carrasco, K. M. Neyman, F. Illas, *Phys. Rev. B* **2007**, *75*, 035115.
[52] K. J. Sun, Y. H. Zhao, H. Y. Su, W. X. Li, *Theor. Chem. Acc.* **2012**, *131*, 1118.